New BIOTECHNOLOGY 83 (2024) 142–154

Contents lists available at ScienceDirect

New BIOTECHNOLOGY

journal homepage: www.elsevier.com/locate/nbt

Production and characterization of novel Anti-HIV Fc-fusion proteins in plant-based systems: *Nicotiana benthamiana* & tobacco BY-2 cell suspension

Noemi Gutierrez-Valdes [a], Francesc Cunyat [b], Juliette Balieu [c], Marie-Laure Walet-Balieu [c,1], Matthew J. Paul [d], Jonas de Groot [a], Amaya Blanco-Perera [b], Jorge Carrillo [b], Patrice Lerouge [c], Mariëlle Jansma-van Seters [a], Jussi J. Joensuu [a,e], Muriel Bardor [c], Julian Ma [d], Julià Blanco [b], Anneli Ritala [a,*]

[a] VTT Technical Research Centre of Finland Ltd, P.O. Box 1000, Espoo FI-02044 VTT, Finland
[b] AlbaJuna Therapeutics SL, Carretera Canyet, Badalona 08916, Spain
[c] Université de Rouen Normandie, Laboratoire GlycoMEV UR4358, SFR Normandie Végétal FED 4277, Innovation Chimie Carnot, Rouen F-76000, France
[d] St George's, University of London, Cranmer Terrace, London SW17 0RE, UK
[e] University of Helsinki, Faculty of Biological and Environmental Sciences, P.O. Box 56, FI-00014 University of Helsinki, Finland

ARTICLE INFO

Keywords:
HIV
Nicotiana benthamiana
BY-2 cell suspension
Plant molecular farming
Hydrophobins
KDEL ER retention signal
Plant-produced biologics glycosylation

ABSTRACT

Multifunctional anti-HIV Fc-fusion proteins aim to tackle HIV efficiently through multiple modes of action. Although results have been promising, these recombinant proteins are hard to produce. This study explored the production and characterization of anti-HIV Fc-fusion proteins in plant-based systems, specifically *Nicotiana benthamiana* plants and tobacco BY-2 cell suspension. Fc-fusion protein expression in plants was optimized by incorporating codon optimization, ER retention signals, and hydrophobin fusion elements. Successful transient protein expression was achieved in *N. benthamiana*, with notable improvements in expression levels achieved through *N*-terminal hydrophobin fusion and ER retention signals. Stable expression in tobacco BY-2 resulted in varying accumulation levels being at highest 2.2.mg/g DW. The inclusion of hydrophobin significantly enhanced accumulation, providing potential benefits for downstream processing. Mass spectrometry analysis confirmed the presence of the ER retention signal and of *N*-glycans. Functional characterization revealed strong binding to CD64 and CD16a receptors, the latter being important for antibody-dependent cellular cytotoxicity (ADCC). Interaction with HIV antigens indicated potential neutralization capabilities. In conclusion, this research highlights the potential of plant-based systems for producing functional anti-HIV Fc-fusion proteins, offering a promising avenue for the development of these novel HIV therapies.

Introduction

HIV, like other retroviruses, integrates its proviral genome into host cells for viral gene transcription and completing its cycle [1]. The activation level of CD4 + T cells during integration influences proviral genome transcription. Highly activated cells support efficient HIV replication, while resting cells show minimal transcription [2]. This leads to the formation of the HIV-1 reservoir, a pool of transcriptionally inactive infected cells shortly after initial infection [3]. These cells are not eliminated by standard HIV treatments and persist throughout the lives of treated HIV-infected individuals.

The primary treatment for HIV is antiretroviral therapy (ART), which involves the administration of a combination of HIV medications aimed at reducing the viral load within the body by targeting different HIV replication stages [4]. ART significantly suppresses HIV to undetectable levels in the blood. However, it is unable to specifically target the latent viral reservoir in HIV-infected patients [5]. This viral reservoir is responsible for viral rebounds after treatment interruptions [6] and thus, turns ART into a chronic, lifelong treatment. There are ongoing efforts to develop treatments for HIV eradication. These include immune activators, therapeutic vaccines, neutralizing antibodies, and antibody derivatives such as Fc-fusion proteins [3,7,8].

Neutralizing antibodies recognizing the HIV-1 envelope glycoprotein (gp120/gp41) have shown a delay in viral rebound after treatment

* Corresponding author.
E-mail address: anneli.ritala@vtt.fi (A. Ritala).
[1] Present Université de Rouen Normandie, INSERM, CNRS, HeRacLeS US51 UAR2026, PISSARO, F-76000 Rouen, France.

https://doi.org/10.1016/j.nbt.2024.08.499
Received 27 February 2024; Received in revised form 9 August 2024; Accepted 9 August 2024
Available online 13 August 2024

interruption [9]. However, monotherapies with these biotherapeutics show rapid viral escape [10]. To avoid that, strategies based on a treatment with a combination of antibodies, or the use of multifunctional antibodies or Fc-fusion proteins have been developed [3].

Essentially, Fc-based fusion proteins combine an IgG Fc domain with another peptide, typically a therapeutic protein or a molecule that interacts with receptors or pathogens [11]. The inclusion of the Fc domain enhances the biological and pharmacological properties of the fused partners, including their ability to bind to Fc receptors on immune cells and prolong the protein's half-life in the bloodstream [12]. The first described CD4-Fc-fusion protein demonstrated inhibitory activity against the formation of syncytia during HIV-1 infection, the most prevalent subtype of HIV [13]. Fc-fusion proteins offer several advantages over other HIV therapeutics. For instance, they can serve as a scaffold for the selection of functional binders or as a carrier for the creation of novel fusion proteins [14].

In the context of the European Pharma-Factory project (https://cordis.europa.eu/project/id/774078), we partnered with AlbaJuna Therapeutics SL, who develops innovative strategies to target HIV and its viral reservoir by designing multifunctional Fc-fusion derivatives. AlbaJuna's biotherapeutics exhibit enhanced antiviral and effector functions against HIV and are conventionally manufactured in mammalian cells (Expi293F, https://www.irsicaixa.es/en/research-and-innovation/spin-offs). Our work aimed to explore the production and functional characterization of AlbaJuna's difficult-to-produce Fc-fusion proteins in plant-based expression systems, with particular emphasis on *Nicotiana benthamiana* and tobacco BY-2 cell suspension. Utilizing *Nicotiana benthamiana* as a transient expression system allowed us to initially validate our expression constructs and address crucial questions concerning protein expression and stability before proceeding to the more complicated BY-2 cell suspension system with stable transformation and integration of encoded genes.

Compared to animal cell-based systems, plant-based systems provide several advantages, including lower capital costs, scalability, reduced risk of contamination with animal pathogens, and potential for glycoengineering [15,16]. Previous studies have utilised both *Nicotiana benthamiana* [17–20] and tobacco BY-2 cell suspension [19,21–23] to produce therapeutics targeting HIV.

The present study aimed to produce AlbaJuna's Fc-fusion proteins in transgenic BY-2 clones using constructs that incorporated various modifications. These modifications included optimizing the codons for *Nicotiana tabacum*, as well as introducing an ER retention signal and the hydrophobin 1 (HFBI) fusion element to potentially enhance protein expression and stability. We ultimately wanted to evaluate the quality and functionality of the proposed anti-HIV Fc-fusion proteins produced in BY-2 suspension cells and compare them to their counterparts produced in mammalian cells. Overall, BY-2 cell suspension showed promise as a platform for producing these anti-HIV Fc-fusion proteins, although further optimization is required.

Materials and methods

Construction of expression vectors

Previous publications [24,25] provided a detailed description of the fundamental structure of the expression vectors used in the present work. In summary, the coding sequences were placed under the regulation of a dual-enhancer Cauliflower mosaic virus 35 S promoter and the soybean *vsp3* terminator. These sequences were flanked by c-myc and Strep II purification tags, as well as a KDEL ER-retention signal. The coding sequences were specifically designed by AlbaJuna (M7AC34, M7AMC34, and M7AMT20) and include two domains of a human CD4 receptor, a native/mutated Fc domain from human IgG1, a $(GGGS)_9$ linker, and a C34/T20 peptide [26–28]. M7AMC34 and M7AMT20 proteins contain mutations [29] in the Fc region to increase affinity for FcγRIIIa (CD16a). To enable expression in plants, the constructs underwent codon optimization for *Nicotiana tabacum*. Initially, three sets of constructs were created, each with different configurations: one with *C*-terminal hydrophobin 1 (HFBI), another with *N*-terminal HFBI, and a third with no HFBI motif. Later, some M7AMC34 constructs were cloned with an additional expression cassette for GFP in the T-DNA as a marker for visual selection of homogeneous transgenic calli. For the constructs containing HFBI, the AlbaJuna molecule (i.e., M7AC34 / M7AMC34 / M7AMT20) and the HFBI were connected by the GAGGGSGGGSGGGSAG linker. Detailed illustrations of these specific configurations can be found in Fig. 1A and Fig. 2B.

Nicotiana benthamiana agroinfiltration

Transient expression was performed as previously described [25]. In summary, the optical density of *Agrobacterium tumefaciens* cultures was adjusted to 1.0, and the suspension was mixed in a 1:1 ratio with *Agrobacterium* containing an expression vector for the p19 suppressor, which prevents post-transcriptional gene silencing [30]. The agroinfiltrated leaves were collected at 6 days post infiltration (dpi) for later extraction and purification.

Transformation and maintenance of the BY-2 culture

The transformation of BY-2 cells was conducted following a previously outlined method [31]. Initially, the BY-2 cultures were maintained as calli on a modified Murashige and Skoog (MS) medium [32] containing 1 % agar and 25 mg/l kanamycin. Every 3–4 weeks, the cultures were subcultured by visually selecting the most fluorescent sections under UV light when visual marker (Green Fluorescent Protein or GFP) was co-transformed. For suspension culture, 50 mL of the modified MS medium supplemented with 50 mg/l kanamycin was used, and the transgenic lines were subcultured on a weekly basis by transferring 5 % (v/v) of the culture to fresh media.

Downstream processing

The BY-2 biomass was collected by centrifugation (10 min, 4000 rpm, room temperature) and freeze-dried for 72 h in a CHRIST ALPHA14 LD plus chamber at a coil temperature of −56 °C. The lyophilised BY-2 biomass was stored at −80 °C until further use. The biomass underwent mechanical disruption using a Retsch mill and steel beads (2 times, 1 min at 29 Hz) (MM301, Haan, Germany).

Protein extraction

The disrupted cell powder was carefully mixed with extraction buffer at a ratio of 30 mL per gram of dry biomass. The extraction buffer used was 1X phosphate-buffered saline with a concentration of 12 mM Na_2HPO_4 * 2 H_2O, 3 mM NaH_2PO_4 *H_2O, and 150 mM NaCl; pH 7.4), along with 1 mM EDTA, 100 mM sodium ascorbate, and 1.12 mL/L of Protease Inhibitor Cocktail (P9599, Sigma Aldrich, St. Louis, MO). To remove insoluble material, the mixture was subjected to centrifugation at 3220 g for 10 min at room temperature (~20 ° C) using an Eppendorf centrifuge 5810 R.

Protein analysis and Western blot

Extracts and purified plant-produced proteins were separated under reducing conditions by SDS-PAGE in a 12 % Bis-Tris gel. Using the Trans-Blot Turbo Transfer System from Bio-Rad, the proteins were subsequently transferred (7 min, 20 V) onto a nitrocellulose membrane.

To detect the Fc-fusion proteins, an anti-IgG Western blotting method was used. The blot was incubated with Goat anti-Human IgG Fc cross-adsorbed secondary antibody DyLight 680 (SA5–10138, Thermo Fisher) diluted 1:10,000, and subsequently visualized using the Odyssey DLs Imaging System (Li-cor). Purified human IgG (3850–1 H-6, Mabtech

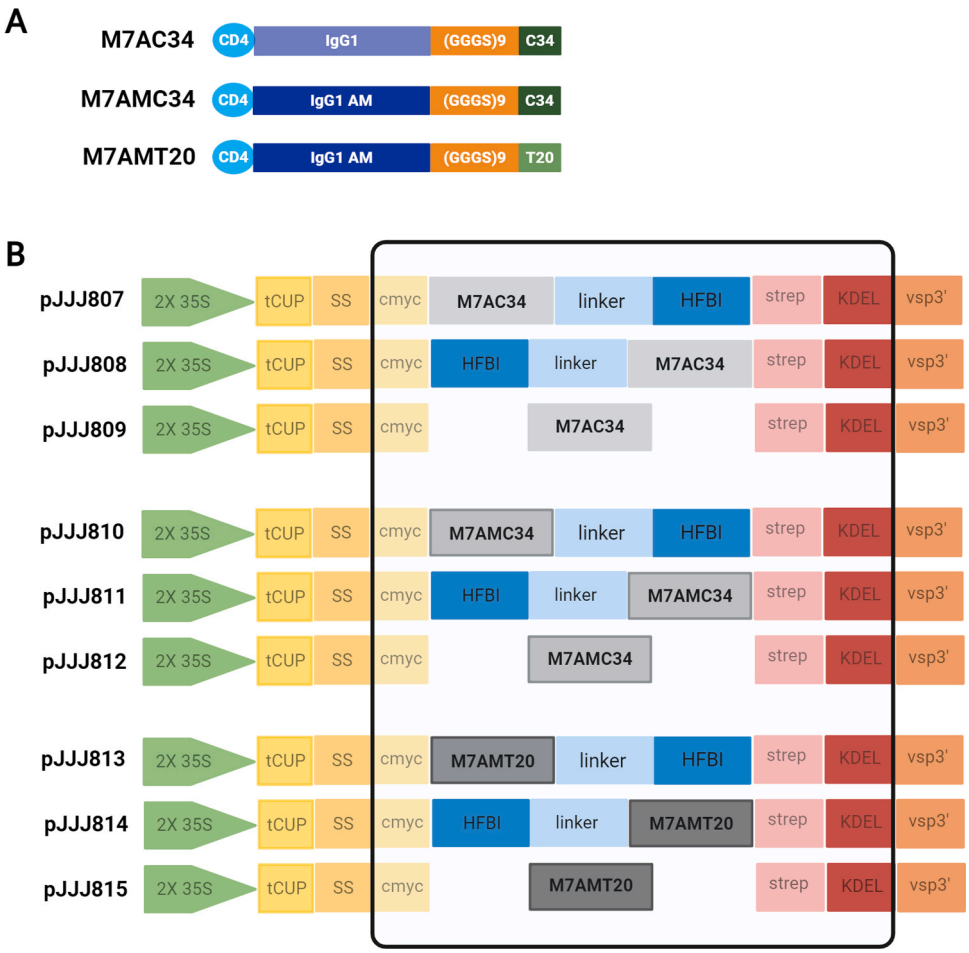

Fig. 1. Novel anti-HIV Fc-fusion protein constructs expressed in plants. **(A)** Configuration of the three Fc-fusion candidates designed by AlbaJuna: M7AC34, M7AMC34, and M7AMT20. These molecules include: CD4, two domains of a human CD4 receptor; IgG1/IgG1M, a native/mutated Fc domain from human IgG1; a $(GGGS)_9$ linker, and a C34/T20 peptide. **(B).** Schematic representation of the anti-HIV Fc encoding gene constructs with or without HFBI for expression to be accomplished in plants: pJJJ807–815. 2X 35 S, dual enhancer Cauliflower mosaic virus 35 S promoter; tCUP, translational enhancer; SS, Pr1bSS; cmyc, c-myc tag; AlbaJuna candidates (M7AC34, M7AMC34, and M7AMT20); linker, GAGGGSGGGSGGGSAG; HFBI, hydrophobin-I; strep, strep-II tag; KDEL, ER retention signal; vsp3', soybean vsp3 terminator.

AB, Sweden) and mammalian cell-based M7AC34 from AlbaJuna were loaded as positive controls. A total soluble protein extract from wild-type BY-2 was used as a background (negative) control.

To detect full sized proteins, anti-c-Myc and StrepII-tags Western blotting methods were employed. The same blot was examined twice using the different specific antibodies. Initially, to detect c-myc in the samples, the blot was subjected to an overnight incubation with the primary antibody c-Myc (A00172, Genscript) diluted 1:1000. Following rinsing, it was incubated for 1 h with the secondary antibody IRdye 680RD Goat anti-Rabbit IgG (926–68071, Li-cor) diluted 1:25,000. Subsequently, the membrane was rinsed again and scanned using the Odyssey DLs Imaging System (Li-cor Biosciences, USA). The following day, the same blot was rinsed and incubated for a minimum of 2 h with the secondary antibody Strep-Tactin AP conjugate (2–1503-001, IBA Lifesciences) diluted 1:2000. After rinsing, it was developed using the BCIP/NBT colour development substrate (S3771, Promega). For visualization, the blot was scanned with the Odyssey DLs Imaging System (Li-cor Biosciences, USA).

ELISA for human IgG binding

Protein extracts were subjected to ELISA analysis for Human IgG (3850–1 H-6, Mabtech AB, Sweden). The ELISA kit was employed following the instructions provided by the manufacturer. Briefly, the kit includes a set of monoclonal antibodies (mAb) specifically designed to bind to the Fc region of human IgG. The capture antibody used in the assay is MT145 (0.5 mg/mL), while the detection antibody is MT78, which has been biotinylated (0.5 mg/mL). Additionally, the kit provides a purified human IgG that served as a standard for comparison and calibration purposes.

Statistical analysis

The statistical analysis was performed on IgG quantification results obtained by ELISA for human IgG binding from *Nicotiana benthamiana* plants infiltrated with the pJJJ810–812, and pNGV001–002. A total of three plants were infiltrated for each construct. The statistical analysis was conducted using SPSS Statistic 22.0 software (IBM, Armonk, NY). The analysis included a one-way ANOVA test to compare the means of the five groups. Following the ANOVA, a Tukey HSD test was performed for post-hoc pairwise comparisons. The significance level was set at 95 %. Tests for normality (Shapiro-Wilk test) and homogeneity of variances (Levene's test) confirmed that the data met the assumptions for ANOVA ($p > 0.05$ for all tests).

Purification through protein A affinity chromatography

The selected plant-produced anti-HIV Fc-fusion proteins were

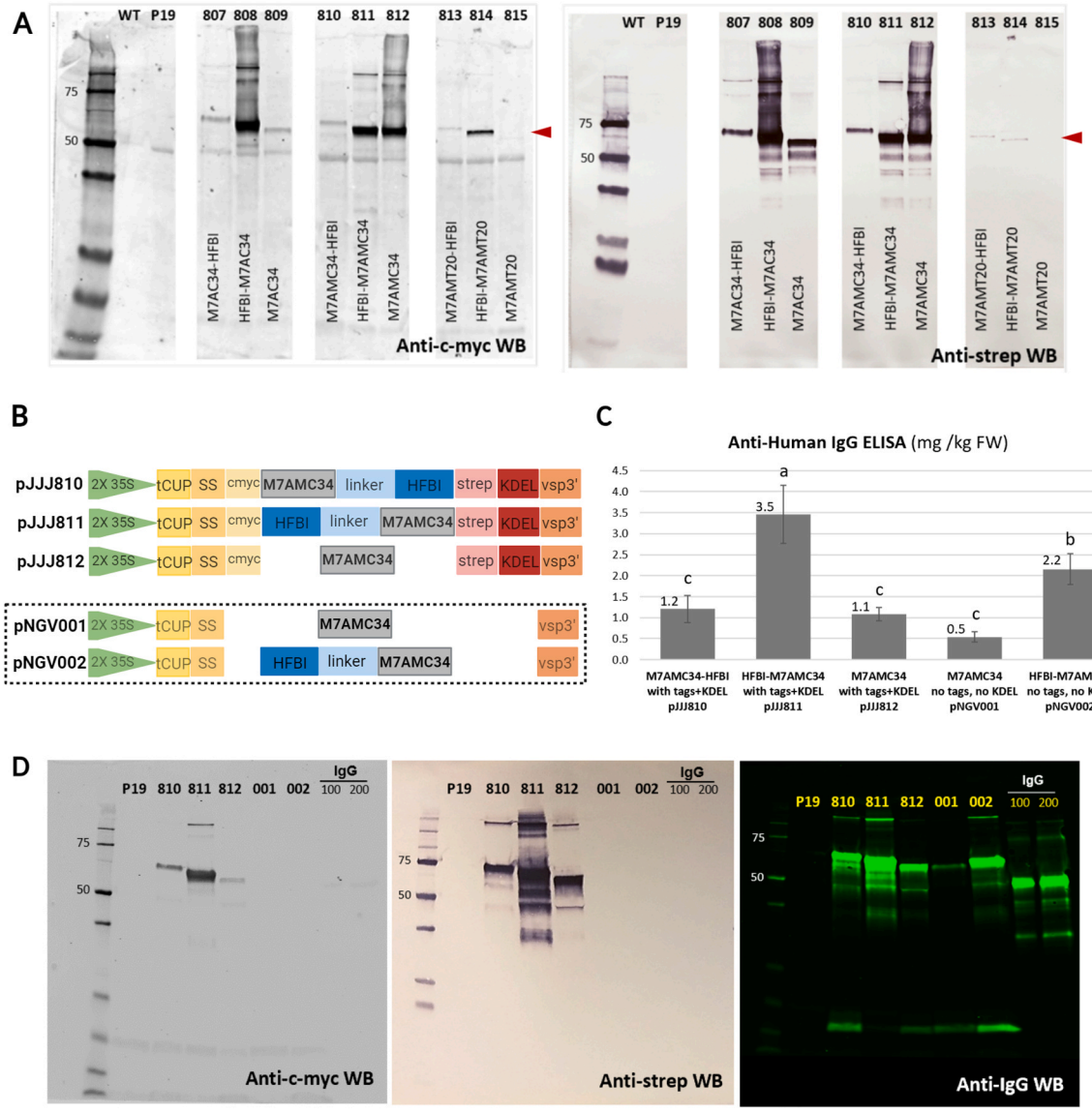

Fig. 2. Anti-HIV Fc-fusion proteins transiently expressed in *Nicotiana benthamiana*. **(A)** Detection in reduced conditions of c-myc- and strep-tags for proteins expressed with encoding constructs: pJJJ807–815. Equal quantities of total soluble protein (TSP) were loaded in each lane (30 µl). TSP from untreated (WT) and P19-portraying Agrobacterium-treated leaves were used as background (negative) controls. The molecular weight of the Fc-fusion proteins containing HFB is 68 kDa and 60 kDa without. **(B)** Configurations of new constructs for the M7AMC34 set. The new constructs, pNGV001 and pNGV002, are marked with a dotted square on the scheme. 2X 35 S, dual enhancer Cauliflower mosaic virus 35 S promoter; tCUP, translational enhancer; SS, Pr1bSS; cmyc, c-myc tag; AlbaJuna candidate (M7AMC34); linker, GAGGGSGGGSGGGSAG; HFBI, hydrophobin-I; strep, strep-II tag; KDEL, ER retention signal; vsp3', soybean vsp3 terminator. **(C)** Human IgG-binding ELISA of TSP extracts from N. benthamiana leaves infiltrated with the constructs on B. Error bars represent standard deviations (n = 3). The letters indicate significant difference between groups ($p < 0.05$). **(D)** Detection in reduced conditions of c-myc- and strep-tags, and human IgG for M7AMC34 set. Equal quantities of total soluble protein (TSP) were loaded in each lane (30 µl). TSP from P19-portraying Agrobacterium-treated leaves was used as a background (negative) control. Human IgG was used as a positive control (100 and 200 ng).

purified using protein A purification. Following protein extraction, the sample underwent clarification through centrifugation at 3000 g for 10 min at 4° C, discarding the pellet. The sample was then diluted 1:10 with 1X cold PBS buffer and passed through a 0.45 µm PES filter. From this stage onward, the sample was consistently kept chilled on ice. Once the AKTA system was prepared and equilibrated, the extract was transferred onto HiTrap Protein A High-Performance Columns [column volume: 1 mL; linear flow rate: 1 mL/min; bed height: 2.5 cm] (GE17–04303-03 Sigma, GE Healthcare, USA). Any unbound and nonspecific proteins attached to the column were washed out using 10 column volumes (CV) of 1X PBS. Elution was carried out by using 5 CVs of 2 M Arginine-HCl at pH 4.7.

ELISA assay for gp140 binding

ELISA plates were coated with UG37 gp140 (5 µg/mL in PBS) (CFAR 0698, NIBSC, UK) and blocked with PBS+ 5 % skimmed milk powder (assay buffer). Fusion proteins were titrated five-fold, along with a negative control (uninfiltrated leaf extract) in assay buffer and incubated at 37 °C for 2 h. Bound fusion protein was detected using an anti-human IgG1 light chain kappa antiserum - HRP (AP015, The Binding Site, UK), diluted 1:2000 in assay buffer. The plates were developed with ready-to-use 3,3',5,5'-Tetramethylbenzidine (TMB Liquid Substrate, Sigma, cat. #T0440) for 5 min and the reaction stopped by the addition of 2 N H_2SO_4. Plates were read on an Tecan Infinite F200 Pro.

SPR assays for assessment of Fc-γRI (CD64) and Fc-γRIII (CD16a) binding

SPR assays were performed using a Biacore X100 instrument (Cytiva, Little Chalfont, UK). CM5 sensor chips were functionalised for antibody binding using the amine coupling kit (Cytiva) to couple protein A (P6031, Merck) to both channels to a final response of 5000 RU. Antibody ligands (M7AMC34-HFBI, HFBI-M7AMC34, M7AC34, and human IgG1k (I5154, Merck)) were captured on the active surface at 240 RU (for FcγRI analysis) or 330RU (for FcγRIIIa). Recombinant human FcγR ectodomains (1257-FC & 4325-FC, R&D) were injected over both flow cells at 25 °C at 40 μl/min for 140 s (for FcγRI analysis) or 60 s (for FcγRIIIa). Surface regeneration was achieved with 2x 90 s injections of 10 mM glycine pH1.5. Kinetic parameters were determined by fitting a 1:1 Langmuir model using the BIAevaluation software (v2.0.1, Cytiva).

Endoprotease digestion

50 μg of M7AMC34-HFBI and HFBI-M7AMC34 proteins were separated on a 12 % (m/v) SDS-PAGE gel. After staining with Coomassie Blue R250, the band corresponding to the purified protein was cut into small pieces and washed several times with a 1/1 (v/v) solution of acetonitrile / 100 mM ammonium bicarbonate pH 8. The protein was then reduced with 100 mM dithiothreitol in ammonium bicarbonate pH 8 for 45 min at 56 °C and then cysteine residues were alkylated with 55 mM iodoacetamide in 100 mM ammonium bicarbonate pH 8 for 30 min at room temperature and in the dark. The gel pieces were then first digested by trypsin (PROMEGA, reference V511A in a ratio 1: 20) in 100 mM ammonium bicarbonate pH 8 and placed at 4 °C for 45 min prior to incubation overnight at 37 °C. The trypsin digestion was stopped by heating at 100 °C for 10 min. Then, the gel pieces were incubated with TLCK-treated chymotrypsin digestion for 3 h (SIGMA, reference C3142, ratio 1: 20) in 100 mM ammonium bicarbonate pH 8 at 37 °C. Peptides and glycopeptides were recovered from the gel pieces by sequential washing with 50 % acetonitrile (v/v), 5 % formic acid (v/v), 100 mM NH_4HCO_3, 100 % acetonitrile (v/v) and finally 5 % formic acid (v/v). The five eluents were combined and then dried down in a SpeedVac centrifuge (Thermo fisher) and store at −20 °C prior to further analyses.

LC-ESI-MS/MS analysis

Analyses of the peptide and glycopeptide mixtures were carried out by nanoLC-ESI-MS/MS on a Q-TOF 6545 XT AdvanceBio mass spectrometer coupled to a nano-LC 1200 liquid chromatography system equipped with an Agilent Zorbax column C18 (150 mm x 75 μm, particle size 5 μm) (Agilent Technologies, Les Ulis, France). Samples were dissolved in acetonitrile/0.1 % formic acid 3/97 v/v and enriched by elution on a RP-C18 40 nL column nano-LC 1200. Peptides and glycopeptides were then separated using a linear gradient from 3 % to 80 % acetonitrile/0.1 % formic acid v/v in 26 min with a flow rate of 350 nL/min. Mass ranges were *m/z* 290 – 2 000 in MS and *m/z* 59 – 3 200 in MS/MS. Data were recorded and treated using Agilent Data Acquisition B.09.00 and Masshunter Qualitative B.07.00 software.

Results

Anti-HIV Fc-fusion proteins adapted to be expressed in plants

AlbaJuna developed three multifunctional Fc-fusion proteins that combine two different HIV-1 Envelope binding sites. The molecules contain a CD4 moiety that binds to the envelope gp120 subunit and a C34 or T20 peptide that binds to the transmembrane gp41 subunit. In addition, some molecules contain a GASDALIE-modified form of the human IgG1 Fc region [29] (later called AM) to increase effector functions (Fig. 1**A**). The design of these proteins enhances their effectiveness and ability to neutralize HIV and to potentially target the *in vivo* viral reservoir. When produced in a mammalian cell system, the AM series show lower production compared to their counterpart with a wild-type Fc region, while T20-derivatives exhibit lower production than the C34-containing molecules (AlbaJuna, unpublished data). Due to these challenges and the advantages offered by plant-based systems, we explored the use of plant expression platforms to produce these proteins. To express the fusion proteins in plants, the proteins were optimized for *Nicotiana tabacum* and engineered to include a *C*-terminal KDEL ER retention signal. Additionally, for each Fc-fusion protein, three different configurations were created: one with a *C*-terminal hydrophobin (HFBI), one with an *N*-terminal HFBI, and one without HFBI. In total, nine constructs were generated. The inclusion of KDEL in all constructs aimed to increase the protein production yield while ensuring protein retention in the ER and the production of high-mannose glycosylation. The HFBI domain was included to assess its impact on the production and functionality of the molecule. These adaptations are illustrated in Fig. 1**B.**

Expression of the candidates in Nicotiana benthamiana

Before expressing the candidates in tobacco BY-2 cell culture, we initially expressed the constructs in *Nicotiana benthamiana* transient expression via agroinfiltration. Based on the results of c-myc and strepII-tag Western blotting, all constructs were successfully expressed with full tagging in *N. benthamiana* transient expression, although there were variations in their accumulation. Interestingly, the constructs with *N*-terminal HFBI showed higher accumulation compared to those with *C*-terminal hydrophobin or no hydrophobin (Fig. 2**A**). To specifically evaluate the effects of KDEL and HFBI, we created two additional versions of the M7AMC34 Fc-fusion protein. One version had no tags (c-myc/strep-tag) or KDEL (pNGV001, later quoted as 001), while the other version had *N*-terminal HFBI but no tags (c-myc/strep-tags) or KDEL (pNGV002, later quoted as 002) (Fig. 2**B**). The original M7AMC34 set (pJJJ810–812, later quoted as 810–812) and the two new constructs (001−002) were then tested in *N. benthamiana* through agroinfiltration to determine which modifications resulted in the highest accumulation of Fc-fusion protein. The construct that yielded the highest Fc-fusion protein accumulation was the one with *N*-terminal HFBI, c-myc and strep-tags, and KDEL (811), which showed a level of 3.5 ± 0.7 mg/kg fresh weight (FW), seven times higher than the lowest accumulation observed in the construct with no tags, no HFBI, and no KDEL (001). The presence of *N*-terminal hydrophobin alone also enhanced protein expression (002), resulting in a level of 2.2 ± 0.4 mg/kg FW, four times higher than the lowest level (001) (Fig. 2**C**). Through anti-myc, anti-strep, and anti-IgG Western blot analysis, we confirmed that the *C*-terminal and *N*-terminal tags were intact in the target proteins expressed with 810–812 encoding constructs, indicating that the proteins were accumulated in full size (Fig. 2**D**).

Activity characterization of N. benthamiana-produced anti-HIV Fc-fusion proteins

The Fc-fusion protein with highest accumulation level reached (HFBI-M7AMC34, 811) and its hydrophobin-free counterpart (M7AMC34, 812) were expressed in *Nicotiana benthamiana* leaves, extracted, purified and their effector functions and neutralization capabilities were assessed. Surface plasmon resonance (SPR) was utilized to determine the binding affinities of these candidates to CD64 and CD16a receptors. The plant-based proteins demonstrated comparable binding affinities to CD64 as the reference (AlbaJuna's M7AC34 produced in Expi293F cells). However, when it came to the CD16a receptor, the plant-based Fc-fusion proteins exhibited approximately four times higher affinity compared to the reference (Fig. 3**A**).

The neutralization capacity of the purified candidates was evaluated using a gp140 binding ELISA. Gp140 is a modified form of the HIV-1 envelope glycoprotein that includes both the gp120 and gp41 subunits

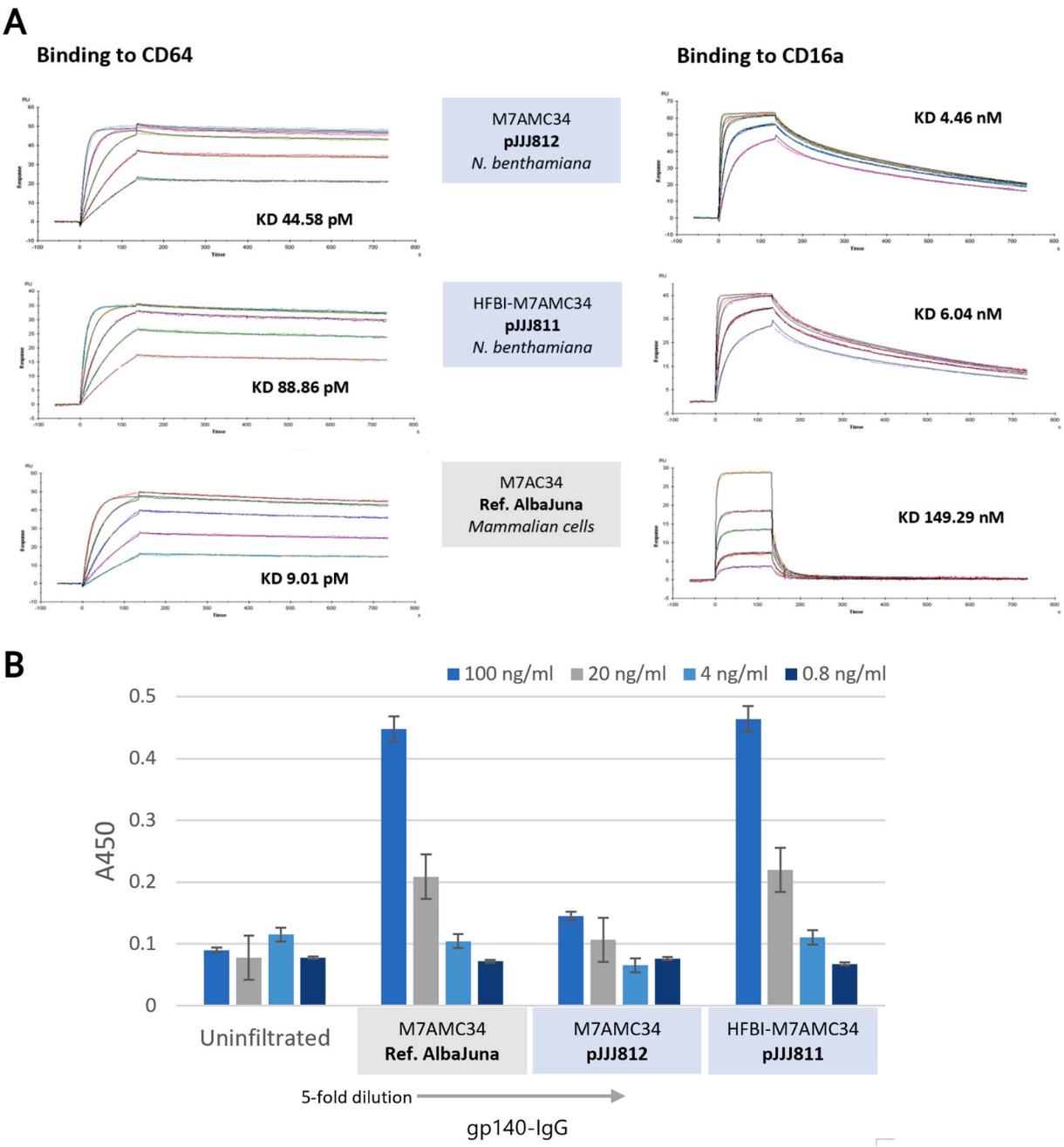

Fig. 3. Activity of *Nicotiana benthamiana*-expressed anti-HIV Fc-fusion proteins. **(A)** Surface plasmon resonance (SPR) analysis of binding to human CD64 and CD16a Fc receptors. The molecules tested were the plant-produced M7AMC34 (pJJJ812) and HFBI-M7AMC34 (pJJJ811), and the mammalian cell-produced M7AC34 as a reference from AlbaJuna. **(B)** Gp140 binding ELISA. Gp140 is a modified form of the HIV envelope glycoprotein that includes both the gp120 and gp41 subunits. The molecules tested were the same as in A, titrated five-fold from 100–0.8 ng/mL. Uninfiltrated leaf protein extract was used as a negative control.

[33]. Binding to gp140 indicates the presence of functional CD4 domain in the Fc-fusion protein. Among the two plant-produced candidates that were examined, the M7AMC34 with *N*-terminal HFBI (811) exhibited the most similar activity to the reference (Fig. 3**B**). The physicochemical characterization and activity assays conducted on the candidates produced in *N. benthamiana* provided evidence that the Fc-fusion proteins could be successfully synthesized in plants thus having potential to similar outcomes when produced in BY-2 cells.

Expression of the candidates in BY-2 cells

Clones of BY-2 cells were generated for all nine constructs (807–815, Fig. 1). In total, 133 BY-2 clones were created and screened for Fc-fusion protein accumulation using ELISA for human IgG binding. The levels of target protein accumulation in BY-2 cells ranged from 0.2–2.2 mg/g dry weight (DW) equivalent to 3.3–38.4 mg/l (Table 1). Over time, some clones kept a baseline level of accumulation, while others completely lost their ability to produce the protein or showed a drastic reduction. This loss of accumulation was attributed to the lack of visual selection during calli subculturing process. To address this issue, new constructs with an additional eGFP visual marker (pNGV003–005, later quoted as 003–005, Fig. 4**A**) were cloned. This time, the focus was solely on the candidate of greatest interest to AlbaJuna, namely M7AMC34 (referring to original constructs of 810–812, Fig. 1). In total, 60 clones were generated with this new set of constructs, which displayed stable growth and comparable yields (ranging from 0.1 to 1.6 mg/g DW equivalent to

Table 1
Tobacco BY-2 transformants and their IgG accumulation levels. The constructs used to generate the clones were pJJJ807–815 (Fig. 1).

Construct	Configuration	Total number of clones	Number of clones expressing protein	Percentage of clones expressing target protein	Highest expression		Number of clones with protein expression	Percentage of clones with protein expression
					(mg/l)*	(mg/g DW)	> 0.5 mg/g DW	> 0.5 mg/g DW
pJJJ807	M7AC34-HFBI	4	2	50	14.0	0.80	1	25
pJJJ808	HFBI-M7AC34	18	15	83	14.0	0.80	2	11
pJJJ809	M7AC34	7	6	86	15.0	0.85	1	14
pJJJ810	M7AMC34-HFBI	21	18	86	29.0	1.65	5	24
pJJJ811	HFBI-M7AMC34	21	17	81	6.0	0.34	0	0
pJJJ812	M7AMC34	21	16	76	11.8	0.67	4	19
pJJJ813	M7AMT20-HFBI	44	41	93	38.4	2.18	10	23
pJJJ814	HFBI-M7AMT20	7	6	86	3.8	0.22	0	0
pJJJ815	M7AMT20	11	3	27	3.3	0.19	0	0

* Estimation was made assuming the dry biomass reaches around 17.6 g/l at the moment of harvesting.

1.8–28.2 mg/l). The IgG accumulation for the top three clones was 1.5, 1.6, and 0.5 mg/g DW for *C*-terminal HFBI M7AMC34 (003), *N*-terminal HFBI M7AMC34 (004), and M7AMC34 (005), respectively (Fig. 4**B**). Although some loss of accumulation occurred over time, it was less pronounced when compared to clones without a visual marker (Fig. 4**C**). The two clones with the highest accumulation, *C*-terminal HFBI M7AMC34 (003_1) and *N*-terminal HFBI M7AMC34 (004_16), were propagated on a larger scale in 400 mL volume. The Fc-fusion protein material was extracted, purified, and further evaluated for activity and glycosylation (Fig. 4**D**).

Activity characterization of BY-2-produced anti-HIV Fc-fusion proteins

The affinity of the candidates for the CD64 and CD16a receptors was measured through surface plasmon resonance (SPR). In general, our candidates exhibited binding affinities that fell within the range of affinities observed for the commercial human IgG1 reference. The binding affinities of the BY-2 produced proteins to CD64 were comparable to the reference, although the plant-produced variants displayed slightly stronger affinities. The equilibrium dissociation constants (KDs) were measured as 94.4 pM for the *C*-terminal HFBI fused protein (M7AMC34-HFBI=*003_1*) and 507.4 pM for the *N*-terminal HFB fused protein (HFBI-M7AMC34 =*004_16*). Similarly, for the CD16a receptor, the plant-produced proteins demonstrated stronger binding affinities, with KDs of 2.6 nM for the *C*-terminal HFBI M7AMC34 and 1.8 nM for the *N*-terminal HFBI M7AMC34 (Fig. 5). For the comparison of *N. benthamiana* produced molecules see Fig. 3**A**.

Glycosylation characterization of BY-2 produced anti-HIV Fc-fusion proteins

The *N*-glycan profiles of the BY2 produced proteins, namely M7AMC34-HFBI and HFBI-M7AMC34, were determined through a glycoproteomic approach [34]. The proteins were successively digested by trypsin and chymotrypsin. The resulting peptide and glycopeptide mixtures were analysed by nano liquid chromatography coupled to electrospray mass spectrometry (LC-ESI-MS/MS). The overall protein sequence coverages were determined to be about 55 %. In their protein sequences, M7AMC34-HFBI and HFBI-M7AMC34 exhibit two *N*-glycosylation sites located respectively on Asn 302 and 512 for M7AMC34-HFBI and on Asn 393 and 603 for HFBI-M7AMC34. These differences in the position of the N-glycosylation sites result from the location of the HFBI motif within the protein sequences. In order to determine the distribution of the *N*-glycans on these two specific *N*-glycosylation sites, the mixtures of peptides and glycopeptides released by the endoprotease digestion were submitted to a targeted LC-ESI-MS/MS analysis [34]. To this end, peptides giving MS/MS spectra exhibiting *N*-glycan diagnostic fragment ions at *m/z* 204 (oxonium ion corresponding to *N*-acetylglucosamine) and 366 (ion corresponding to the disaccharide motif Man-GlcNAc) were selected as being glycopeptides. Numerous MS/MS spectra assigned to glycopeptides were extracted from LC-ESI-MS/MS data generated for endoproteases digests of both M7AMC34-HFBI and HFBI-M7AMC34 proteins. Their glycan sequences were then determined by analysis of the glycan fragment ions. As illustration, the doubly charged $[M+2H]^{2+}$ ion at *m/z* 1177.94 was assigned to $E_{509}INNY_{513}$ from M7AMC34-HFBI *N*-linked to a $Man_8GlcNAc_2$ (Man-8) oligomannoside (Fig. 6**A**). In the MS/MS spectrum, in addition to diagnostic ions at 204.09 and 366.14, fragment ions were assigned to the peptide carrying a chitobiose unit and one to five mannose residues. Fig. 6**B** shows the MS/MS spectrum and the fragment ion assignments of the doubly charged $[M+2H]^{2+}$ ions of $E_{389}EQYNSTYR_{397}$ from HFBI-M7AMC34 *N*-linked to a GnM_3XGn_2 complex *N*-glycan which refers as a core $Man_3GlcNAc_2$ *N*-glycan bearing a terminal GlcNAc residue and a β(1,2)-xylose motif linked to the β-Man.

Based on fragmentation ion patterns of glycopeptides selected by the targeted LC-ESI-MS/MS analysis, oligomannose and complex plant *N*-glycans were identified on the two *N*-glycosylation sites of M7AMC34-HFBI and HFBI-M7AMC34 and their relative percentages were calculated based on their molecular ion intensities in the LC-ESI-MS/MS analysis. Table 2 reports on the glycan distribution per *N*-glycosylation site for both M7AMC34-HFBI and HFBI-M7AMC34.

Discussion

In our work, we have explored the production of multifunctional anti-HIV Fc-fusion proteins in plant-based systems. The candidate proteins, originally designed by AlbaJuna, are typically manufactured in mammalian cells, and engineered to exhibit neutralizing activity and enhanced ADCC activities for preventing HIV infection and viral entry. To produce these Fc-fusion proteins in plants, we performed codon optimization for *Nicotiana tabacum* expression, incorporated a *C*-terminal KDEL sequence to retain the proteins in the endoplasmic reticulum (ER) ensuring a consistent high-mannose glycosylation, and introduced HFBI at either the *N*-terminus or *C*-terminus to potentially enhance protein production and stability (Fig. 1).

Our primary objective was to characterize the production of these proteins in tobacco BY-2 cell suspension system. However, we first utilized transient *Nicotiana benthamiana* as a platform for protein expression to validate our expression constructs. This choice allowed us to address crucial questions that were subsequently adopted using the BY-2

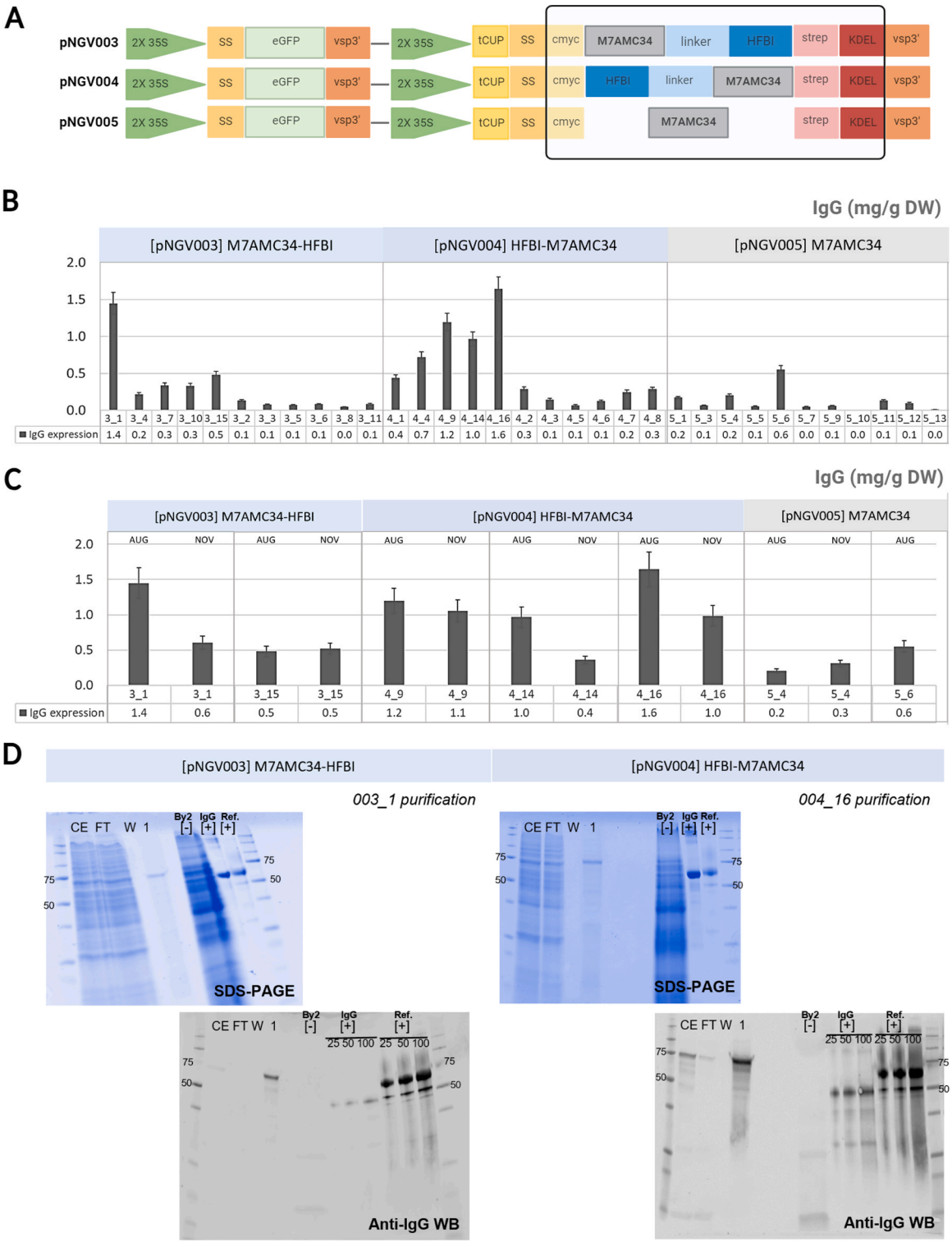

Fig. 4. Anti-HIV Fc-fusion proteins expressed in tobacco BY-2 cells. **(A)** New constructs for the M7AMC34 Fc-fusion proteins set with eGFP as a visual marker (pNGV003–005). 2X 35 S, dual enhancer Cauliflower mosaic virus 35 S promoter; tCUP, translational enhancer; SS, Pr1bSS; eGFP, enhanced green fluorescent protein; cmyc, c-myc tag; AlbaJuna candidate (M7AMC34); linker, GAGGGSGGGSGGGSAG; HFBI, hydrophobin-I; strep, strep-II tag; KDEL, ER retention signal; vsp3', soybean vsp3 terminator. **(B)** Human IgG binding ELISA analysis of TSP extracts from 33 BY-2 transformants generated with the constructs on A. **(C)** IgG accumulation levels (assessed through ELISA) for the best BY-2 clones of each encoding construct after establishment of stable BY-2 clones and after 3 months of subculturing regime. **(D)** Reduced SDS-PAGE gels and Western blots for human IgG detection after Protein A purification from extracts of the transgenic 003_1 and 004_16 carrying BY-2 clones. The expected molecular weight of our Fc-fusion proteins is 68 kDa. CE=crude extract; FT=flow through; W=washing; 1 =purified product. Wild-type BY-2 soluble protein was used as a background (negative) control. For CE, FT, W, 1 and the negative control, each lane was loaded with 30uL of the corresponding sample. Human IgG from the ELISA kit was used as a positive control (IgG 25, 50, 100 ng). AlbaJuna's M7AC34 produced in mammalian cells was used as a reference control (Ref 25,50,100 ng).

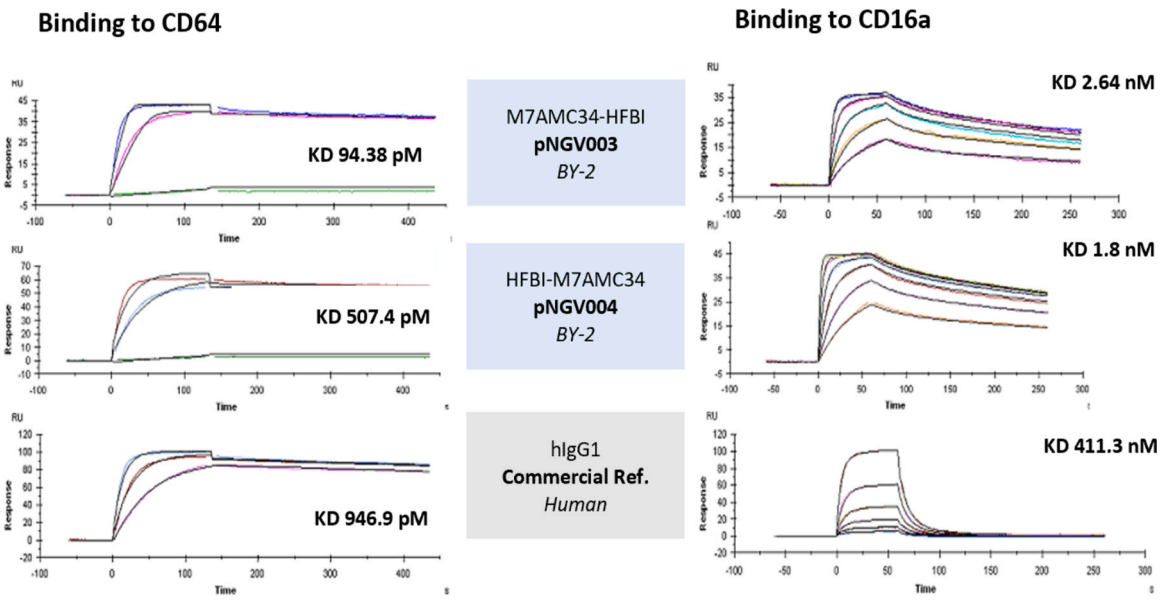

Fig. 5. Activity of BY-2-expressed anti-HIV Fc-fusion proteins. Surface plasmon resonance (SPR) analysis of binding to human CD64 and CD16a Fc receptors. The molecules tested were the BY-2 produced M7AMC34-HFBI (003) and HFBI-M7AMC34 (004), and a commercially available human IgG1.

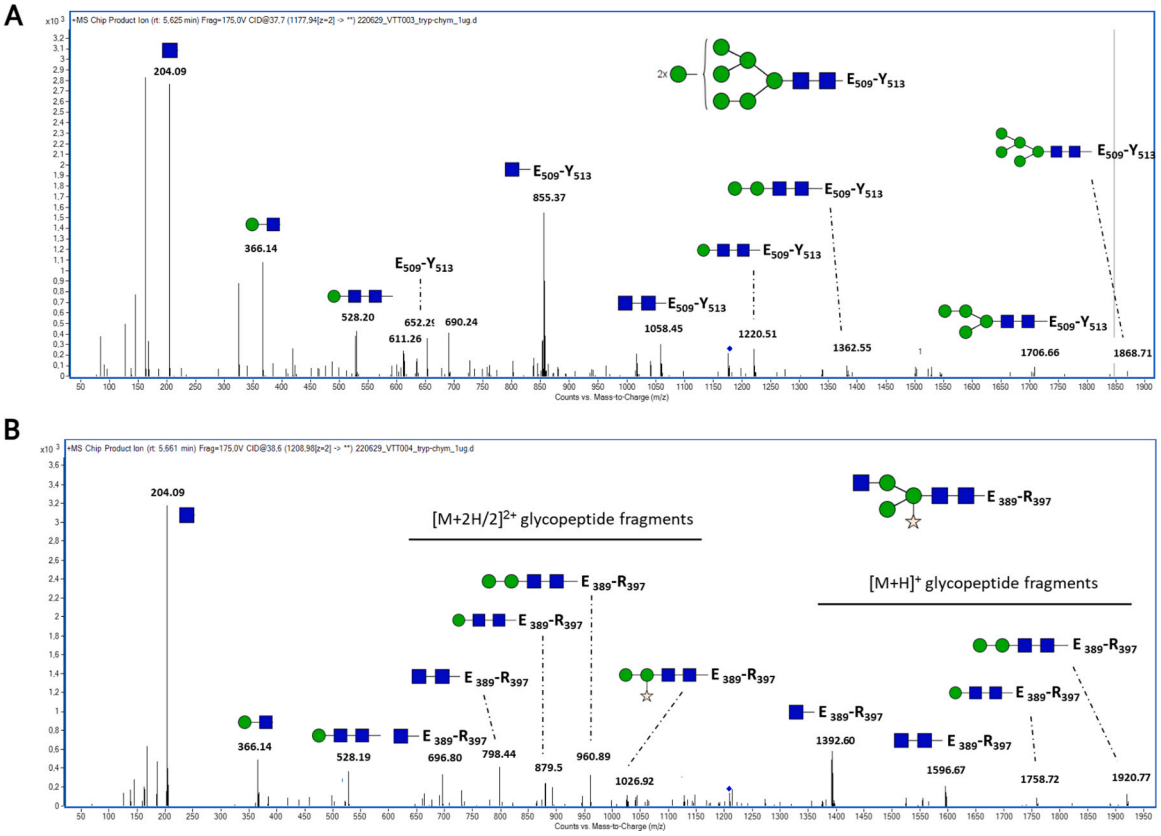

Fig. 6. Examples of N-glycan profiling of the BY-2 produced M7AMC34-HFBI and HFBI-M7AMC34 Fc-fusion proteins. A glycoproteomic approach combined with nano-LC-ESI-MS/MS analysis was performed for analysing the N-glycosylation sites and glycan distributions. Upon digestion of the proteins with a combination of trypsin and chymotrypsin, peptide and glycopeptide mixtures were generated prior to their analyses using nano-LC-ESI-MS/MS. The glycopeptides were identified using a targeted search based on N-glycan diagnostic ions. MS/MS spectra of **(A)** the doubly charged [M+ 2 H]2 + ion at *m/z* 1177.94 assigned to $E_{509}INNY_{513}$ from M7AMC34-HFBI N-linked to Man-8 and **(B)** the doubly charged [M+ 2 H]2 + ions at *m/z* 1208.98 assigned $E_{389}EQYNSTYR_{397}$ from HFBI-M7AMC34 N-linked to GnM3XGn2. GlcNAc: blue square; Man: green circle and Xyl: yellow star.

Table 2
Glycan distribution per N-glycosylation site for the BY-2 produced M7AMC34-HFBI and HFBI-M7AMC34. Each protein exhibits two distinct glycosylation sites: Asn 302 and Asn 512 for M7AMC34-HFBI, and Asn 393 and Asn 603 for HFBI-M7AMC34. The relative percentages represent the proportion of each glycan type based on their molecular ion intensities in the targeted LC-ESI-MS/MS analysis of M7AMC34-HFBI (003_1) and HFBI-M7AMC34 (004_16).

M7AMC34-HFBI (003_1)						
Glycosite	Peptide sequence	Calculated peptide $[M+H]^+$	Observed peptide $[M+H]^+$	Observed glycopeptide $[M+2H]^{2+}$	Glycan	%
302	R.EEQYNSTYR.V	1189.51	1189.83	1365.52	Man−7	9.09
302	R.EEQYNSTYR.V	1189.51	1189.49	1445.05	Man−8	90.91
512	R.EINNY.T	652.29	652.29	1177.97	Man−8	100
HFBI-M7AMC34 (004_16)						
Glycosite	Peptide sequence	Calculated peptide $[M+H]^+$	Observed peptide $[M+H]^+$	Observed glycopeptide $[M+2H]^{2+}$	Glycan	%
393	R.EEQYNSTYR.V	1189.51	1189.50	1142.14	GnM_3Gn_2	29.09
393	R.EEQYNSTYR.V	1189.51	1189.50	1208.98	GnM_3XGn_2	14.55
393	R.EEQYNSTYR.V	1189.51	1189.49	1366.04	Man−7	23.64
393	R.EEQYNSTYR.V	1189.51	1189.51	1446.83	Man−8	32.73
603	R.EINNY.T	652.29	652.29	1096.41	Man−7	100

cell suspension expression system with stable transformation and integration of encoded genes.

The effect of KDEL and HFBI on the recombinant protein accumulation

In *N. benthamiana*, all initial constructs (pJJJ807–pJJJ815) were successfully expressed, displaying varying levels of accumulation in the leaves. Constructs containing *N*-terminal HFBI showed higher accumulation compared to other variants (Fig. 2**A**). Furthermore, when examining the specific impact of c-myc and strap tags, HFBI, and KDEL in the constructs (pJJJ810–811 and pNGV001–002) (Fig. 2**C**–**D**), we observed that the fusion of the protein with *N*-terminal hydrophobin and the inclusion of a KDEL ER retention signal had an additive effect on protein accumulation. *N*-terminal HFBI fusion demonstrated the most significant increase in accumulation. However, some research groups [25,35] have shown that for some proteins, the *C*-terminal HFBI appeared to have a stronger influence on the recombinant protein accumulation in *N. benthamiana*. The reasons why HFBI tags enhance accumulation for certain fusion partners [25,36–39] but not for others [40] are not fully understood. In our case, regardless of its position, the inclusion of HFBI resulted in an average 2.4 to 7-fold increase in accumulation compared to the partner protein without hydrophobin. Moreover, targeting the recombinant proteins to the ER through the KDEL signal also contributed to higher accumulation, which has also been observed with other proteins [41–47]. It is worth mentioning that the overexpression of some proteins in the ER can lead to necrotic lesions on agroinfiltrated *N. benthamiana* leaves as early as 4 days post-infiltration (dpi) [25]. However, in our study, the accumulation of the Fc-fusion proteins did not cause any harm to the leaves, which remained healthy even until 10 dpi (data not presented).

In the BY-2 system, the expression of the constructs exhibited high variability (Table 1 and Fig. 4**B**). This is a common occurrence inherent to the BY-2 transformation process [48]. The variability in transformation outcomes can be attributed to several factors, including the positioning of the T-DNA insert, the number of T-DNA copies integrated into the genome, and the epigenetic state of the integration site. For example, a higher number of T-DNA copies can lead to increased expression levels, while the epigenetic state of the integration site can impact transgene expression, as gene silencing can be influenced by DNA methylation and histone modifications [49].

Even though the use of GFP facilitated the initial identification of transgenic calli during the screening process, many of the callus lines still exhibited heterogeneous expression patterns after multiple passages. This heterogeneity was evident when transgenic clones carrying a visual GFP marker were observed under UV light, the presence of fluorescent green patches alongside the typical yellow hue of BY-2 cells was evident. This phenomenon has been previously observed and attributed to a heterogeneous population of cells, with varying levels of fluorescence intensity ranging from high, moderate, to non-expressing cells, and only careful subculturing over 20 passages resulted in homogenous lines [50]. This heterogeneity explains why our BY-2 suspension cultures displayed variable expression over time and a decline in Fc-fusion protein accumulation over continuous passages (Fig. 4**C**). As mentioned earlier, both genetic and epigenetic factors can contribute to the inconsistency in productivity within the BY-2 system. Previous studies have attempted to mitigate the heterogeneity of BY-2 cultures by generating monoclonal lines [51,52]. While these lines exhibited consistent expression levels for extended periods, ranging from several months [51] to up to a year [52], they were still susceptible to somaclonal variation [53] and epigenetic changes such as gene silencing. Therefore, cryopreservation and periodic repetition of the clone selection process may be necessary, although monoclonal cultures are crucial for meeting industrial requirements for consistent batch-to-batch production and specific characterization of production lines [54].

Regarding the hydrophobin impact in BY-2 cells, we observed that the accumulation levels in our clones transformed with hydrophobin-fused constructs were 2.4–4.4 times higher compared to those without hydrophobin. Although there was variation in accumulation among the clones, we noticed a consistent trend of higher accumulation in proteins fused with hydrophobin, particularly when the hydrophobin was fused at the *N*-terminus (Fig. 4**B**). Hydrophobins have been shown to promote recombinant protein accumulation by facilitating the synthesis of protein bodies (PBs) in both *N. benthamiana* [25,39] and BY-2 [24,55] systems. PBs are compact, spherical structures that originate from the endoplasmic reticulum and are thought to assemble once a certain threshold of recombinant protein is reached. The fusion of recombinant proteins with hydrophobin increases the likelihood of PB formation [38]. It is possible that PBs were formed in both *N. benthamiana* and BY-2 clones in our experiments. The formation of PBs in our BY-2 clones could be advantageous for exploring alternative methods of Fc-fusion protein recovery, such as aqueous two-phase separation (ATPS), which has the potential to facilitate downstream processing and reduce purification costs.

While the incorporation of hydrophobin and the KDEL signal for ER retention has contributed to increased accumulation of our Fc-fusion proteins, the low productivity of the BY-2 production platform remains a challenge. However, there are several possible approaches available to enhance the system. These approaches include the generation of monoclonal lines [51], the use of improved culture media [21,56] clone screening based on fluorescence-activated cell sorting [52] and the development of protease knock out lines [57].

The effect of KDEL and HFBI on the recombinant protein functionality

AlbaJuna's design of the M7AMC34 Fc-fusion protein aimed to enhance its effector functions by engineering its Fc domain to interact

with the CD64 and CD16a binding sites. Engagement of the Fc domain with these Fc gamma receptors, CD16a (FcγRIIIA) and CD64 (FcγRI), respectively, triggers important biological activities such as antibody-dependent cellular cytotoxicity (ADCC) and antibody-dependent cellular phagocytosis (ADCP) mediated by immune cells [58]. In addition to incorporating the Fc domain, the M7AMC34 was also engineered to interact bi-specifically with two regions of the HIV-1 envelope protein (gp120 and gp41) through its CD4 and C34 domains. The CD4 domain binds to gp120, a glycoprotein responsible for receptor attachment and virus-cell membrane fusion [14]. The C34 domain binds to gp41, another glycoprotein that anchors gp120 to the viral membrane and facilitates the fusion of viral and cellular membranes [59]. The interaction between HIV and the M7AMC34 is expected to inhibit the attachment of the virus to host CD4 + T cells, thus preventing infection. Additionally, it interferes with the conformational changes necessary for membrane fusion, thereby impeding viral entry into host cells.

The binding affinities of the Fc-fusion proteins produced in *N. benthamiana* and BY-2 cells to CD64 and were comparable to those of the candidate produced in mammalian cells and stronger than a commercial human IgG reference (Fig. 5). Supplementary Table 1 presents all the kinetic parameters of molecular binding and dissociation of the plant based anti-HIV Fc-fusion proteins and references with the CD64 and CD16a receptors via SPR. In our analysis of the *N. benthamiana* produced molecules, we found that the fusion of hydrophobin (HFBI-M7AMC34) did not significantly affect the binding affinities of the recombinant protein compared to the partner without hydrophobin (M7AMC34) (Fig. 3**A**). Thus, we conclude that the hydrophobin fusion, specifically when fused at the N-terminus, does not appear to impact the Fc receptor binding capacity of the candidate. For the BY-2 produced molecules, we directly compared two candidates with *C*-terminally and *N*-terminally fused hydrophobin. Both molecules showed similar binding affinities to CD16a. However, it was noteworthy that the *C*-terminally fused HFBI molecule (M7AMC34-HFBI) exhibited a 5-fold stronger binding affinity to CD64 than its partner (Fig. 5). In comparison to the human cell-produced IgG1 reference, our plant-produced proteins displayed a higher affinity for the CD16a receptor (with KDs of 2.64 and 1.8 nM for M7AMC34-HFBI and the HFBI-M7AMC34 respectively versus a KD of 411.3 nM for the reference). This result was expected given that the AM candidates contain GASDALIE-type mutations that enhance the binding to the CD16a receptor. Since CD16a is involved in antibody-dependent cellular cytotoxicity (ADCC) mediated by natural killer (NK) cells [60], we hypothesize that the plant-based Fc-fusion proteins may have higher efficacy in ADCC activity rather than inducing CD64-mediated phagocytosis. However, further cell-based interaction assays are needed to confirm this hypothesis.

Although we did not directly assess the HIV neutralization capability of our plant-produced Fc-fusion proteins, we conducted a gp140-IgG ELISA to evaluate their interactions (Fig. 3**B**). The gp140 protein consists of gp120 and gp41 linked by a disulfide bond [61], allowing us to approximate the interactions involving CD4. These ELISA results showed positive binding for the HFBI-M7AMC34, indicating interactions similar to those observed with the AlbaJuna reference. Based on this, we infer that the plant-based Fc-fusions are likely to exhibit a comparable neutralization activity to their counterparts manufactured in mammalian cells. However, it is essential to confirm the HIV neutralization efficacy of our plant-based Fc-fusion proteins in future viral studies using different HIV clades.

To our knowledge, there have been no clinical trials involving recombinant proteins fused to hydrophobins, limiting our understanding of potential HFBI toxicity. Nevertheless, preclinical studies with hydrophobins like SC3 and SC4 have shown no cytotoxic or immunogenic effects [62,63] indicating their safety in medical applications. Furthermore, since hydrophobins are derived from food sources and are consumed by humans through the consumption of mushrooms and fungus-fermented foods, they may be considered non-toxic [64]. Hydrophobins have also shown to extend the half-life of their fusion partners, as seen with the Glucagon Like Peptide-1 (GLP-1)- HGFI hydrophobin complex, which experienced a six-fold increase in serum half-life in comparison with GLP-1 alone, benefiting the treatment of type 2 diabetes by extending insulin activity [65]. This example illustrates the potential stabilizing effects of hydrophobins as fusion partners in general. Nevertheless, further assays are needed to assess safety and toxicity of the HFBI fusion on the anti-HIV Fc-fusion protein candidates.

Our analysis of glycosylation in the BY-2 produced Fc-fusion proteins revealed the presence of two glycosylation sites in both M7AMC34-HFBI and HFBI-M7AMC34 as expected according to the amino acid sequence. These sites were located in the same regions as the corresponding protein produced in mammalian cells, with one site in the Fc domain and the other in the C34 binding site region, also as expected. Regarding the complexity of the glycosites, in M7AMC34-HFBI the KDEL tag resulted in an efficient retention in the ER as demonstrated by the identification of only Man-7 and Man-8 oligomannosides *N*-linked to the two *N*-glycosylation sites as reported in the literature [66,67]. However, for HFBI-M7AMC34, the identification of partially maturated *N*-glycans GnM and GnMX indicated less efficiency of the *C*-terminal KDEL retrieving signal since these complex glycans resulted from maturations of ER oligomannosides in the late and medium plant Golgi apparatus. Moreover, the differences of the glycan profiles between on Asn 393 and 603 *N*-glycosylation sites of HFBI-M7AMC34 suggested that these two sites exhibit different accessibility to Golgi maturation enzymes due to the overall protein 3D structure (Table 2). We hypothesize that the proximity of the hydrophobin to the KDEL signal may have resulted in a stabilizing effect for ER retention. Thus, the closer the hydrophobin was to the KDEL signal, the more efficient the retention of the protein in the ER was. The glycosylation sites in the Fc region of all the proteins predominantly exhibited high mannose content, which did not adversely affect the antibody-dependent cellular cytotoxicity (ADCC) activity, unlike some similar proteins produced in plants [17,20]. We do not anticipate significant functional issues related to viral neutralization due to glycosylation at the C34 binding site. When comparing the glycosylation of our BY-2 produced protein to the mammalian cell-produced counterpart, the latter is more structurally complex but still maintains its ADCC activity without impairment (AlbaJuna, personal communication).

Conclusions

In our pursuit of developing plant-based anti-HIV Fc-fusion proteins, key findings on productivity and functionality have emerged from our expression approaches. Regarding productivity, incorporating hydrophobin (HFBI) into *Nicotiana benthamiana* and tobacco BY-2 cell suspension systems significantly improved protein accumulation, regardless of HFBI positioning. Protein accumulation was further enhanced when combined with the *C*-terminal KDEL ER retention signal, without adverse effects on plant health. Productivity, particularly in tobacco BY-2 cells, exhibited inherent variability. Strategies like generating monoclonal lines and refining culture conditions are essential for consistent and reliable protein production. In addition to our findings, understanding challenges like genetic instability and the role of the 35 S promoter can be crucial for optimizing plant-based protein production [68]. Further research must consider these factors to ensure efficiency and reliability in the plant-based expression systems.

Regarding functionality, plant-produced anti-HIV Fc-fusion proteins showed binding affinities to CD64 and CD16a receptors comparable to their mammalian-produced counterparts. Notably, a significantly higher affinity for the CD16a receptor suggests potential enhancement in antibody-dependent cellular cytotoxicity (ADCC) against HIV infection. Glycosylation patterns in the Fc region were predominantly high mannose, with no detrimental effects on functionality, particularly in ADCC activity. Variations in glycosylation site positions are not expected to substantially influence the viral neutralization capacity. However, this needs to be confirmed in HIV neutralization assays.

Altogether, these findings indicate that plant-based Fc-fusion proteins maintain functionality and hold promise for anti-HIV therapeutics.

In summary, modification approaches using hydrophobin and the KDEL signal offer potential to enhance productivity and functionality of plant-based anti-HIV Fc-fusion proteins. These findings support the feasibility of plant-based expression systems for biotherapeutics with improved properties, particularly in HIV treatment and eradication efforts. Further refinement and exploration of these strategies may lead to more effective and economically viable anti-HIV therapies. Our current protein level ~4 mg/kg is not sufficient for industrial application just yet, as the product concentration should be in g/l ranges to become attractive for industrial production.

CRediT authorship contribution statement

Patrice Lerouge: Writing – review & editing, Validation, Investigation, Formal analysis. **Jorge Carrillo:** Writing – review & editing, Validation, Investigation, Formal analysis. **Amaya Blanco-Perera:** Writing – review & editing, Validation, Investigation, Formal analysis. **Jonas de Groot:** Writing – review & editing, Validation, Investigation, Formal analysis. **Muriel Bardor:** Writing – review & editing, Supervision, Funding acquisition, Conceptualization. **Noemi Gutierrez-Valdes:** Writing – review & editing, Writing – original draft, Visualization, Validation, Investigation, Formal analysis. **Jussi J. Joensuu:** Writing – review & editing, Supervision. **Anneli Ritala:** Writing – review & editing, Writing – original draft, Validation, Supervision, Investigation, Funding acquisition, Formal analysis, Conceptualization. **Mariëlle Jansma-van Seters:** Writing – review & editing, Validation, Investigation, Formal analysis. **Matthew J. Paul:** Writing – review & editing, Visualization, Validation, Supervision, Project administration, Investigation, Funding acquisition, Formal analysis, Conceptualization. **Marie-Laure Walet-Balieu:** Writing – review & editing, Validation, Investigation, Formal analysis. **Julià Blanco:** Writing – review & editing, Supervision, Project administration, Funding acquisition, Conceptualization. **Juliette Balieu:** Writing – review & editing, Visualization, Validation, Investigation, Formal analysis. **Julian Ma:** Writing – review & editing, Supervision, Project administration, Funding acquisition, Conceptualization. **Francesc Cunyat:** Writing – review & editing, Visualization, Validation, Investigation, Formal analysis.

Declaration of Competing Interest

JC and JB were founders of AlbaJuna Therapeutics. AB, JB, JC and FC were employees of AlbaJuna therapeutics. Other authors, no conflicts of interest.

Acknowledgements

This research was funded by the European Union's Horizon 2020 Research and Innovation Program, specifically through the PharmaFactory project under grant agreement No. 774078. The authors also wish to acknowledge the valuable technical assistance provided by Jaana Rikkinen, Kaisa Rinta-Harri, and Tuuli Teikari from VTT. Furthermore, the University of Rouen Normandie's support is gratefully acknowledged. The glycoanalysis work received financial backing from the French government through the ANR agency, both under the Grand Défi Bioproduction and Biologics (ANR-21-F2II-0005) and the ANR PRCE DAGENTA project (ANR-21-CE20-0038-001).

Appendix A. Supporting information

Supplementary data associated with this article can be found in the online version at doi:10.1016/j.nbt.2024.08.499.

References

[1] Furtado MR, Callaway DS, Phair JP, Kunstman KJ, Stanton JL, Macken CA, et al. Persistence of HIV-1 transcription in peripheral-blood mononuclear cells in patients receiving potent antiretroviral therapy. N Engl J Med 1999;340:1614–22. https://doi.org/10.1056/NEJM199905273402102.

[2] Pierson T, McArthur J, Siliciano RF. Reservoirs for HIV-1: mechanisms for viral persistence in the presence of antiviral immune responses and antiretroviral therapy. Annu Rev Immunol 2000;18:665–708. https://doi.org/10.1146/ANNUREV.IMMUNOL.18.1.665.

[3] Carrillo J, Clotet B, Blanco J. Antibodies and antibody derivatives: new partners in HIV eradication strategies. Front Immunol 2018;9:2429. https://doi.org/10.3389/FIMMU.2018.02429/BIBTEX.

[4] Madzime M, Rossouw TM, Theron AJ, Anderson R, Steel HC. Interactions of HIV and antiretroviral therapy with neutrophils and platelets. Front Immunol 2021;12:634386. https://doi.org/10.3389/FIMMU.2021.634386/BIBTEX.

[5] Siliciano JD, Kajdas J, Finzi D, Quinn TC, Chadwick K, Margolick JB, et al. Long-term follow-up studies confirm the stability of the latent reservoir for HIV-1 in resting CD4+ T cells. 2003;9 Nat Med 2003;9(6):727–8. https://doi.org/10.1038/NM880.

[6] Chun TW, Davey RT, Engel D, Lane HC, Fauci AS. Re-emergence of HIV after stopping therapy. 1999;401 Nature 1999;401(6756):874–5. https://doi.org/10.1038/44755.

[7] Caskey M, Klein F, Nussenzweig MC. Broadly neutralizing anti-HIV-1 monoclonal antibodies in the clinic. 2019;25 Nat Med 2019;25(4):547–53. https://doi.org/10.1038/S41591-019-0412-8.

[8] Deeks SG, Archin N, Cannon P, Collins S, Jones RB, de Jong MAWP, et al. Research priorities for an HIV cure: International AIDS Society Global Scientific Strategy 2021. 2021;27 Nat Med 2021;27(12):2085–98. https://doi.org/10.1038/s41591-021-01590-5.

[9] Scheid JF, Horwitz JA, Bar-On Y, Kreider EF, Lu CL, Lorenzi JCC, et al. HIV-1 antibody 3BNC117 suppresses viral rebound in humans during treatment interruption. 2016;535 Nature 2016;535(7613):556–60. https://doi.org/10.1038/NATURE18929.

[10] Shingai M, Nishimura Y, Klein F, Mouquet H, Donau OK, Plishka R, et al. Antibody-mediated immunotherapy of macaques chronically infected with SHIV suppresses viraemia. 2013;503 Nature 2013;503(7475):277–80. https://doi.org/10.1038/NATURE12746.

[11] Czajkowsky DM, Hu J, Shao Z, Pleass RJ. Fc-fusion proteins: new developments and future perspectives. EMBO Mol Med 2012;4:1015–28. https://doi.org/10.1002/EMMM.201201379.

[12] Cao W, Piedmonte DM, Ricci MS, Yeh PY. Formulation, drug product, and delivery: considerations for Fc-fusion proteins. In: Ryll T, Chamow S, Lowman H, Farson D, editors. Therapeutic Fc-Fusion Proteins. 1st ed. John Wiley & Sons, Incorporated; 2014. p. 115–53. https://doi.org/10.1002/9783527675272.ch05.

[13] Yang C, Gao X, Gong R. Engineering of Fc fragments with optimized physicochemical properties implying improvement of clinical potentials for Fc-based therapeutics. Front Immunol 2018;8:1860. https://doi.org/10.3389/FIMMU.2017.01860/BIBTEX.

[14] Shubin Z, Li W, Poonia B, Ferrari G, LaBranche C, Montefiori D, et al. An HIV envelope gp120-Fc fusion protein elicits effector antibody responses in rhesus macaques. Clin Vaccin Immunol 2017;24. https://doi.org/10.1128/CVI.00028-17.

[15] Sack M, Rademacher T, Spiegel H, Boes A, Hellwig S, Drossard J, et al. From gene to harvest: insights into upstream process development for the GMP production of a monoclonal antibody in transgenic tobacco plants. Plant Biotechnol J 2015;13:1094–105. https://doi.org/10.1111/pbi.12438.

[16] Buyel JF. Towards a seamless product and process development workflow for recombinant proteins produced by plant molecular farming. Biotechnol Adv 2024;75:108403. https://doi.org/10.1016/J.BIOTECHADV.2024.108403.

[17] Hamorsky KT, Kouokam JC, Dent MW, Grooms TN, Husk AS, Hume SD, et al. Engineering of a lectibody targeting high-mannose-type glycans of the HIV envelope. Mol Ther 2019;27:2038–52. https://doi.org/10.1016/J.YMTHE.2019.07.021.

[18] Puchol-Tarazona A, Paireder M, Taubenschmid Y, Maresch D, Mach L. Degradation of anti-HIV antibodies 2F5 and PG9 by proteases of Nicotiana benthamiana. N Biotechnol 2018;44:S26. https://doi.org/10.1016/J.NBT.2018.05.132.

[19] Mandal MK, Fischer R, Schillberg S, Schiermeyer A. Inhibition of protease activity by antisense RNA improves recombinant protein production in Nicotiana tabacum cv. Bright Yellow 2 (BY-2) suspension cells. Biotechnol J 2014;9:1065–73. https://doi.org/10.1002/biot.201300424.

[20] Stelter S, Paul MJ, Teh AYH, Grandits M, Altmann F, Vanier J, et al. Engineering the interactions between a plant-produced HIV antibody and human Fc receptors. Plant Biotechnol J 2020;18:402–14. https://doi.org/10.1111/PBI.13207.

[21] Holland T, Sack M, Rademacher T, Schmale K, Altmann F, Stadlmann J, et al. Optimal nitrogen supply as a key to increased and sustained production of a monoclonal full-size antibody in BY-2 suspension culture. Biotechnol Bioeng 2010;107:278–89. https://doi.org/10.1002/BIT.22800.

[22] Sack M, Paetz A, Kunert R, Bomble M, Hesse F, Stiegler G, et al. Functional analysis of the broadly neutralizing human anti-HIV-1 antibody 2F5 produced in transgenic BY-2 suspension cultures. FASEB J 2007;21:1655–64. https://doi.org/10.1096/FJ.06-5863COM.

[23] Mandal MK, Kronenberger T, Zulka MI, Windshügel B, Schiermeyer A. Structure-based discovery of small molecules improving stability of human broadly-neutralizing anti-HIV antibody 2F5 in plant suspension cells. Biotechnol J 2022;17:2100266. https://doi.org/10.1002/BIOT.202100266.

[24] Reuter LJ, Bailey MJ, Joensuu JJ, Ritala A. Scale-up of hydrophobin-assisted recombinant protein production in tobacco BY-2 suspension cells. Plant Biotechnol J 2014;12:402–10. https://doi.org/10.1111/PBI.12147.
[25] Joensuu JJ, Conley AJ, Lienemann M, Brandle JE, Linder MB, Menassa R. Hydrophobin fusions for high-level transient protein expression and purification in nicotiana benthamiana. Plant Physiol 2010;152:622. https://doi.org/10.1104/PP.109.149021.
[26] Qi Z, Shi W, Xue N, Pan C, Jing W, Liu K, et al. Rationally designed anti-HIV peptides containing multifunctional domains as molecule probes for studying the mechanisms of action of the first and second generation HIV fusion inhibitors. J Biol Chem 2008;283:30376–84. https://doi.org/10.1074/JBC.M804672200.
[27] Lazzarin A, Clotet B, Cooper D, Reynes J, Arasteh K, Nelson M, et al. Efficacy of enfuvirtide in patients infected with drug-resistant HIV-1 in Europe and Australia. N Engl J Med 2003;348:2186–95. https://doi.org/10.1056/NEJMOA035211.
[28] Lalezari JP, Henry K, O'hearn M, Montaner JSG, Piliero PJ, Walmsley S, et al. Enfuvirtide, an HIV-1 fusion inhibitor, for drug-resistant HIV infection in North and South America. N Engl J Med 2003;348:2175–85. https://doi.org/10.1056/NEJMOA035026.
[29] Ahmed AA, Keremane SR, Vielmetter J, Bjorkman PJ. Structural characterization of GASDALIE Fc bound to the activating Fc receptor FcγRIIIa. J Struct Biol 2016;194:78–89. https://doi.org/10.1016/J.JSB.2016.02.001.
[30] Silhavy D, Molnár A, Lucioli A, Szittya G, Hornyik C, Tavazza M, et al. A viral protein suppresses RNA silencing and binds silencing-generated, 21- to 25-nucleotide double-stranded RNAs. EMBO J 2002;21:3070–80. https://doi.org/10.1093/EMBOJ/CDF312.
[31] De Sutter V., Vanderhaeghen R., Tilleman S., Lammertyn F., Vanhoutte I., Karimi M., et al. Exploration of jasmonate signalling via automated and standardized transient expression assays in tobacco cells n.d. https://doi.org/10.1111/j.1365–313X.2005.02586.x.
[32] Nagata T, Kumagai F. Plant cell biology through the window of the highly synchronized tobacco BY-2 cell line. Methods Cell Sci 1999;21:123–7. https://doi.org/10.1023/A:1009832822096.
[33] Scheid JF, Mouquet H, Feldhahn N, Walker BD, Pereyra F, Cutrell E, et al. A method for identification of HIV gp140 binding memory B cells in human blood. J Immunol Methods 2008;343:65–7. https://doi.org/10.1016/j.jim.2008.11.012.
[34] Balieu J, Jung JW, Chan P, Lomonossoff GP, Lerouge P, Bardor M. Investigation of the N-glycosylation of the SARS-CoV-2 S protein contained in VLPs produced in nicotiana benthamiana. Molecules 2022;27:5119. https://doi.org/10.3390/MOLECULES27165119/S1.
[35] Reuter LJ, Bailey MJ, Joensuu JJ, Ritala A. Scale-up of hydrophobin-assisted recombinant protein production in tobacco BY-2 suspension cells. Plant Biotechnol J 2014;12:402–10. https://doi.org/10.1111/pbi.12147.
[36] Phan HT, Hause B, Hause G, Arcalis E, Stoger E, Maresch D, et al. Influence of elastin-like polypeptide and hydrophobin on recombinant hemagglutinin accumulations in transgenic tobacco plants. PLoS One 2014;9:e99347. https://doi.org/10.1371/JOURNAL.PONE.0099347.
[37] Jacquet N, Navarre C, Desmecht D, Boutry M. Hydrophobin fusion of an influenza virus hemagglutinin allows high transient expression in nicotiana benthamiana, easy purification and immune response with neutralizing activity. PLoS One 2014;9:e115944. https://doi.org/10.1371/JOURNAL.PONE.0115944.
[38] Saberianfar R, Joensuu JJ, Conley AJ, Menassa R. Protein body formation in leaves of Nicotiana benthamiana: a concentration-dependent mechanism influenced by the presence of fusion tags. Plant Biotechnol J 2015;13:927–37. https://doi.org/10.1111/PBI.12329.
[39] Reuter L, Ritala A, Linder M, Joensuu J. Novel hydrophobin fusion tags for plant-produced fusion proteins. PLoS One 2016;11:e0164032. https://doi.org/10.1371/JOURNAL.PONE.0164032.
[40] Pereira EO, Kolotilin I, Conley AJ, Menassa R. Production and characterization of in planta transiently produced polygalacturanase from Aspergillus niger and its fusions with hydrophobin or ELP tags. BMC Biotechnol 2014;14:1–11. https://doi.org/10.1186/1472-6750-14-59/FIGURES/6.
[41] Schouten A, Rossien J, Van Engelen FA, De Jong GA, Borst-Vrenssen AW, Zilverentant JF, et al. The C-terminal KDEL sequence increases the expression level of a single-chain antibody designed to be targeted to both the cytosol and the secretory pathway in transgenic tobacco. Plant Mol Biol 1996;30:781–93. https://doi.org/10.1007/BF00019011/METRICS.
[42] Fiedler U, Phillips J, Artsaenko O, Conrad U. Optimization of scFv antibody production in transgenic plants. Immunotechnology 1997;3:205–16. https://doi.org/10.1016/S1380-2933(97)00014-6.
[43] Ramirez N, Ayala M, Lorenzo D, Palenzuela D, Herrera L, Doreste V, et al. Expression of a single-chain Fv antibody fragment specific for the hepatitis B surface antigen in transgenic tobacco plants. Transgenic Res 2002;11:61–4. https://doi.org/10.1023/A:1013967705337/METRICS.
[44] Conley AJ, Mohib K, Jevnikar AM, Brandle JE. Plant recombinant erythropoietin attenuates inflammatory kidney cell injury. Plant Biotechnol J 2009;7:183–99. https://doi.org/10.1111/J.1467-7652.2008.00389.X.
[45] Conley AJ, Joensuu JJ, Menassa R, Brandle JE. Induction of protein body formation in plant leaves by elastin-like polypeptide fusions. BMC Biol 2009;7:48. https://doi.org/10.1186/1741-7007-7-48/FIGURES/7.
[46] Huang Z, Dry I, Webster D, Strugnell R, Wesselingh S. Plant-derived measles virus hemagglutinin protein induces neutralizing antibodies in mice. Vaccine 2001;19:2163–71. https://doi.org/10.1016/S0264-410X(00)00390-X.
[47] Menassa R, Nguyen V, Jevnikar A, Brandle J. A self-contained system for the field production of plant recombinant interleukin-10. Mol Breed 2001;8:177–85. https://doi.org/10.1023/A:1013376407362/METRICS.
[48] Nagata T. Hidden history of the tobacco BY-2 cell line. J Plant Res 2023;136:781. https://doi.org/10.1007/S10265-023-01490-4.
[49] Gelvin SB. Integration of Agrobacterium T-DNA into the plant genome. Annu Rev Genet 2017;51:195–217. https://doi.org/10.1146/ANNUREV-GENET-120215-035320.
[50] Häkkinen ST, Reuter L, Nuorti N, Joensuu JJ, Rischer H, Ritala A. Tobacco BY-2 media component optimization for a cost-efficient recombinant protein production. Front Plant Sci 2018;9:45. https://doi.org/10.3389/FPLS.2018.00045/BIBTEX.
[51] Nocarova E, Fischer L. Cloning of transgenic tobacco BY-2 cells; an efficient method to analyse and reduce high natural heterogeneity of transgene expression. BMC Plant Biol 2009;9:1–11. https://doi.org/10.1186/1471-2229-9-44/FIGURES/5.
[52] Kirchhoff J, Raven N, Boes A, Roberts JL, Russell S, Treffenfeldt W, et al. Monoclonal tobacco cell lines with enhanced recombinant protein yields can be generated from heterogeneous cell suspension cultures by flow sorting. Plant Biotechnol J 2012;10:936–44. https://doi.org/10.1111/j.1467-7652.2012.00722.x.
[53] James EA, Wang C, Wang Z, Reeves R, Shin JH, Magnuson NS, et al. Production and characterization of biologically active human GM-CSF secreted by genetically modified plant cells. Protein Expr Purif 2000;19:131–8. https://doi.org/10.1006/prep.2000.1232.
[54] Santos RB, Abranches R, Fischer R, Sack M, Holland T. Putting the spotlight back on plant suspension cultures. Front Plant Sci 2016;7:297. https://doi.org/10.3389/FPLS.2016.00297/BIBTEX.
[55] Kurppa K, Reuter LJ, Ritala A, Linder MB, Joensuu JJ. In-solution antibody harvesting with a plant-produced hydrophobin–protein A fusion. Plant Biotechnol J 2018;16:404–14. https://doi.org/10.1111/PBI.12780.
[56] Matoba N, Fuqua JL, Mason HS, Häkkinen ST, Reuter L, Nuorti N, et al. Tobacco BY-2 media component optimization for a cost-efficient recombinant protein production. Front Plant Sci 2018;9:45. https://doi.org/10.3389/fpls.2018.00045.
[57] Mandal MK, Fischer R, Schillberg S, Schiermeyer A. Inhibition of protease activity by antisense RNA improves recombinant protein production in Nicotiana tabacum cv. Bright Yellow 2 (BY-2) suspension cells. Biotechnol J 2014;9:1065–73. https://doi.org/10.1002/BIOT.201300424.
[58] de Taeye SW, Rispens T, Vidarsson G. The ligands for human IgG and their effector functions. 2019;8:30 Antibodies 2019;Vol 8:30. https://doi.org/10.3390/ANTIB8020030.
[59] Guttman M, Lee KK. A functional interaction between gp41 and gp120 is observed for monomeric but not oligomeric, uncleaved HIV-1 Env gp140. J Virol 2013;87:11462–75. https://doi.org/10.1128/JVI.01681-13/SUPPL_FILE/ZJV999098188SO1.PDF.
[60] Hullsiek R, Li Y, Snyder KM, Wang S, Di D, Borgatti A, et al. Examination of IgG Fc receptor CD16A and CD64 expression by canine leukocytes and their ADCC activity in engineered NK cells. Front Immunol 2022;13:566. https://doi.org/10.3389/FIMMU.2022.841859/BIBTEX.
[61] Kovacs JM, Noeldeke E, Ha HJ, Peng H, Rits-Volloch S, Harrisona SC, et al. Stable, uncleaved HIV-1 envelope glycoprotein gp140 forms a tightly folded trimer with a native-like structure. Proc Natl Acad Sci USA 2014;111:18542–7. https://doi.org/10.1073/PNAS.1422269112/SUPPL_FILE/PNAS.201422269SI.PDF.
[62] Janssen MI, Van Leeuwen MBM, Scholtmeijer K, Van Kooten TG, Dijkhuizen L, Wösten HAB. Coating with genetic engineered hydrophobin promotes growth of fibroblasts on a hydrophobic solid. Biomaterials 2002;23:4847–54. https://doi.org/10.1016/S0142-9612(02)00240-5.
[63] Janssen MI, Van Leeuwen MBM, Van Kooten TG, De Vries J, Dijkhuizen L, Wösten HAB. Promotion of fibroblast activity by coating with hydrophobins in the β-sheet end state. Biomaterials 2004;25:2731–9. https://doi.org/10.1016/j.biomaterials.2003.09.060.
[64] Wösten HAB, Scholtmeijer K. Applications of hydrophobins: current state and perspectives. Appl Microbiol Biotechnol 2015;99:1587–97. https://doi.org/10.1007/s00253-014-6319-x.
[65] Zhao L, Xu H, Li Y, Song D, Wang X, Qiao M, et al. Novel application of hydrophobin in medical science: a drug carrier for improving serum stability. Sci Rep 2016;6. https://doi.org/10.1038/SREP26461.
[66] Sriraman R, Bardor M, Sack M, Vaquero C, Faye L, Fischer R, et al. Recombinant anti-hCG antibodies retained in the endoplasmic reticulum of transformed plants lack core-xylose and core-α(1,3)-fucose residues. Plant Biotechnol J 2004;2:279–87. https://doi.org/10.1111/J.1467-7652.2004.00078.X.
[67] Triguero A, Cabrera G, Cremata JA, Yuen CT, Wheeler J, Ramírez NI. Plant-derived mouse IgG monoclonal antibody fused to KDEL endoplasmic reticulum-retention signal is N-glycosylated homogeneously throughout the plant with mostly high-mannose-type N-glycans. Plant Biotechnol J 2005;3:449–57. https://doi.org/10.1111/J.1467-7652.2005.00137.X.
[68] Navarre C, Orval R, Peeters M, Bailly N, Chaumont F. Issue when expressing a recombinant protein under the control of p35S in Nicotiana tabacum BY-2 cells. Front Plant Sci 2023;14:1266775. https://doi.org/10.3389/FPLS.2023.1266775/BIBTEX.